

# Effect of interpolation on specular reflections in texture-based automatic colonic polyp detection

Rukiye Nur Kaçmaz<sup>1,2</sup>  | Bülent Yılmaz<sup>1,2,3</sup>  | Zafer Aydın<sup>1,4</sup> 

<sup>1</sup>Electrical and Computer Engineering Department, Graduate School of Engineering and Sciences, Abdullah Gül University, Kayseri, Turkey

<sup>2</sup>Biomedical Image and Signal Analysis Laboratory, Abdullah Gül University, Kayseri, Turkey

<sup>3</sup>Electrical and Electronics Engineering Department, School of Engineering, Abdullah Gül University, Kayseri, Turkey

<sup>4</sup>Computer Engineering Department, School of Engineering, Abdullah Gül University, Kayseri, Turkey

## Correspondence

Rukiye Nur Kaçmaz, Electrical and Computer Engineering Department, Graduate School of Engineering and Sciences, Abdullah Gül University, Kayseri, Turkey.

Email: rukiyenurkacmaz@gmail.com

## Abstract

Reflections of LED light cause unwanted noise effects called specular reflection (SR) on colonoscopic images. The aim of this study was to seek answers to the following two questions. (a) How are the texture features used in automatic detection of polyps affected by the interpolation on specular reflections? (b) If they are affected does it really affect the classification performance? In order to answer these questions, we used 610 colonoscopy images, and divided each image into tiles whose sizes were 32-by-32 pixels. From these tiles, we selected the ones without any specular reflection. We added different shape and size specular reflections cropped from real images onto the reflection-free tiles. We then used the nearest neighbors, bilinear and bicubic interpolation techniques on the tiles on which SRs were added. On these tiles we extracted 116 texture features using 3 second-order approaches, and 4 first-order statistics. First, we used paired sample *t* test. Second, we performed automatic classification of polyps and background using random forest and *k* nearest neighbors (*k*-NN) approaches using the texture features for different combinations of specular reflections added on the tiles from the polyp or background. The results showed that depending on the size of specular reflection, interpolation can cause a significant difference between the texture features that were coming from reflection-free tiles and the same tiles on which interpolation was performed. In addition, we note that bicubic interpolation may be preferred to eliminate specular reflection when texture features are used for background and polyp discrimination.

## KEYWORDS

classification, colon polyp, image processing, machine learning, specular reflection

## 1 | INTRODUCTION

Colon cancer (CC) develops in large intestine which is the last part of the digestive system. Many colon cancer cases begin with adenomatous polyps called small and benign cells.<sup>1</sup> Adenomatous polyps refer to abnormal growth of the tissue. Studies show that CC is usually caused by pre-existing adenomatous polyps.<sup>2</sup> According to the study of the American Cancer Society, CC is the third

most common type of deadly cancer. Most CCs are composed of “silent” tumors. These are slow-growing tumors that generally do not give any indication until they reach a large size. CC can be prevented and treated if it is diagnosed early.<sup>3</sup> Therefore, the polyps that the specialists detect are removed from the patient regardless of whether they are malignant or benign so as not to create future risk. The imaging system used for this procedure is called “colonoscopy.” Colonoscopy allows examination of

the intestines with the light and camera on the tip, but also the removal of polyp with the help of the catheter at the end. Colonoscopy is an operator-dependent process; thus, attention deficiency or fatigue of the operator can cause missed polyps. The polyps which are not detected early enough can turn into a cancerous structure, and after many years the disease can be diagnosed as an advanced cancer, in which the survival rate is lower than 10%.<sup>4</sup> In addition to the colonoscopy systems, in recent years, wireless capsule endoscopy (WCE) has been developed for human-independent computer-aided screening. In this method, the camera is placed in a vitamin-sized capsule. As this capsule travels along the digestive tract, thousands of images are captured by the recorder connected to the patient's waist. Although this procedure seems more advantageous for the patient, it is not very efficient in terms of examining about 60 000 images. The examination and processing of these images is very time consuming; it has not yet become a preferred method.<sup>1</sup>

Computer-aided polyp detection for colonoscopic and WCE images can be performed according to the polyp shape or texture. In the literature, there are many studies focusing on shape-based<sup>5-9</sup> and texture-based polyp detection. Shape-based polyp detection generally uses geometrical shape, appearance or boundaries of polyps.<sup>5,10,11</sup> Texture is one of the most important characteristics used to describe the region of interest in image. They are the measures of intensity variation of a surface that determine properties such as smoothness, roughness, and regularity. Previous works on colonoscopic images show that texture-based methods are more popular. For example, Wang et al used local binary pattern (LBP) approach,<sup>12</sup> Tjoa et al employed color histogram and texture spectral features,<sup>13</sup> and Alexandre et al proposed a method using color space features.<sup>14</sup> In addition to these studies, the texture analysis approach like gray level co-occurrence matrix (GLCM) was preferred in numerous publications.<sup>15-17</sup> These approaches use pixel intensities on the images. In order to get reliable results, quality of the image should also be high. The quality can be deteriorated by the light reflections, date or patient name information on the colonoscopic images. Especially, reflections of light which occurs due to the LED light source used to illuminate the scene to visually examine the colon cause unwanted noise effects called "specular reflection." These undesired reflections occur on the polyp or other colon tissue, and affect the texture features obtained from the image. In order to perform texture-based polyp detection successfully the effect of specular reflection should be minimized. Previously, several researchers proposed approaches to eliminate reflection on mages. For example, Guo et al suggested a method to eliminate specular reflection for endoscopic images. In

that study, they proposed two steps: (a) Detection of reflection using thresholding and (b) elimination of reflection using an inpainting algorithm.<sup>18</sup> Among other methods proposed in the literature, Stehle used spectral deconvolution algorithm to remove reflections,<sup>19</sup> Arnold et al<sup>20</sup> and Karapetyan et al<sup>21</sup> preferred inpainting algorithms which can also be called as an interpolation technique. In general, image interpolation approaches compute new values for pixels whose intensity values are saturated due to specular reflection using adjacent/surrounding pixels that have normal intensity values. As it has many types, in this study we used three different interpolation methods: bilinear, nearest neighbor and bicubic interpolation.

In machine learning literature, texture-based automatic detection of colonic polyps involves extracting texture features from the images or parts of images (subimages) and applying classification techniques on these features to discriminate whether it includes a polyp structure or not. The aim of this study was to seek answers to the following two questions. (a) How are the texture features used in automatic detection of polyps affected by the interpolation on specular reflections? (b) If they are affected by the interpolation approach does it really affect the classification performance? In order to answer these questions, we used 610 colonoscopy images, and divided each image into tiles whose sizes were 32-by-32 pixels. From these tiles, we selected the ones without any kind or size of specular reflection, because we wanted to add different shape and size "real" specular reflections onto the reflection-free tiles. Therefore, we were able to investigate the changes in texture features on the reflection-free tiles and the reflection-added and interpolated tiles. By the term "real specular reflections added" we mean that they were cropped from the tiles with reflections and pasted on the reflection-free tiles randomly. The interpolation approaches we used were the nearest neighbors, bilinear and bicubic interpolation. For answering the second question, we used *t* test to investigate whether these interpolation methods caused any difference in terms of classification performance to discriminate polyps from the colon background. We performed automatic classification of polyps and background using random forest and k nearest neighbors (k-NN) approaches.

## 2 | MATERIALS AND METHODS

### 2.1 | Colonoscopy images

In this study, we employed colonoscopy images coming from the "CVC-ClinicDB" database prepared in the

Hospital Clinic of Barcelona, Spain.<sup>22</sup> The images of this database were acquired using white light conventional colonoscopy system. It is the official database used in the training stages of MICCAI 2015 Sub-Challenge on Automatic Polyp Detection Challenge in Colonoscopy Videos. The dataset includes 610 colonoscopic images which were obtained from 29 patients. Approximately 20 to 25 images were obtained from different angles from each patient. Each image contains polyps in different shapes, size, and numbers. In addition, ground truth images showing the location of the polyps were provided. Sample polyp and ground truth images are given in Figure 1.<sup>22</sup>

## 2.2 | Preprocessing

The size of the images used in this study was  $288 \times 384$  (Figure 2A). Because, the images include black parts on the edges that do not contain any information, we selected a rectangle from the initial images to result in  $224 \times 192$  images (Figure 2B) to be used in the subsequent phases of our study. First, we have converted these images into gray scale. For analysis and labeling purposes, we, then, divided each image into  $32 \times 32$  squares which we referred to as “tiles.” We obtained a total of 42 tiles from each image (Figure 2C). In the final phase of this study, which we discussed later in this manuscript, we automatically classified/discriminated healthy and polyp tissues. In that phase, we only needed tiles that

contained pure healthy and pure polyp tissues. However, as shown in Figure 2C, several tiles included both healthy and polyp tissues, such as tiles numbered as 10, 19, and 23. If tiles were pure healthy, that is, there were no pixels corresponding to polyps or specular reflections, these tiles were labeled as healthy. For tiles with specular reflections reader should refer to Figure 2D. It shows that there are spots that correspond to the specular reflection on some of the tiles like tile 21 and 27. Likewise, if a tile was labeled as pure polyp, that means there were no pixels corresponding to specular reflections or healthy tissues. For the determination of polyp tissue, we used ground truth images and logic operations, and for the specular reflections, we used a simple thresholding approach. As a result of this process, we obtained a total of 15 674 tiles from 610 images. The number of tiles that were labeled as polyp and healthy was 1426 and 14 248, respectively.

## 2.3 | Addition of specular reflections to tiles

In order to investigate the effect of specular reflections on polyp detection we added real reflections on tiles labeled as pure polyp and pure healthy. By real reflections, we mean that we selected four different size “actual reflections” from tiles that contained specular reflections (which were not pure tiles). Figure 3 shows four real

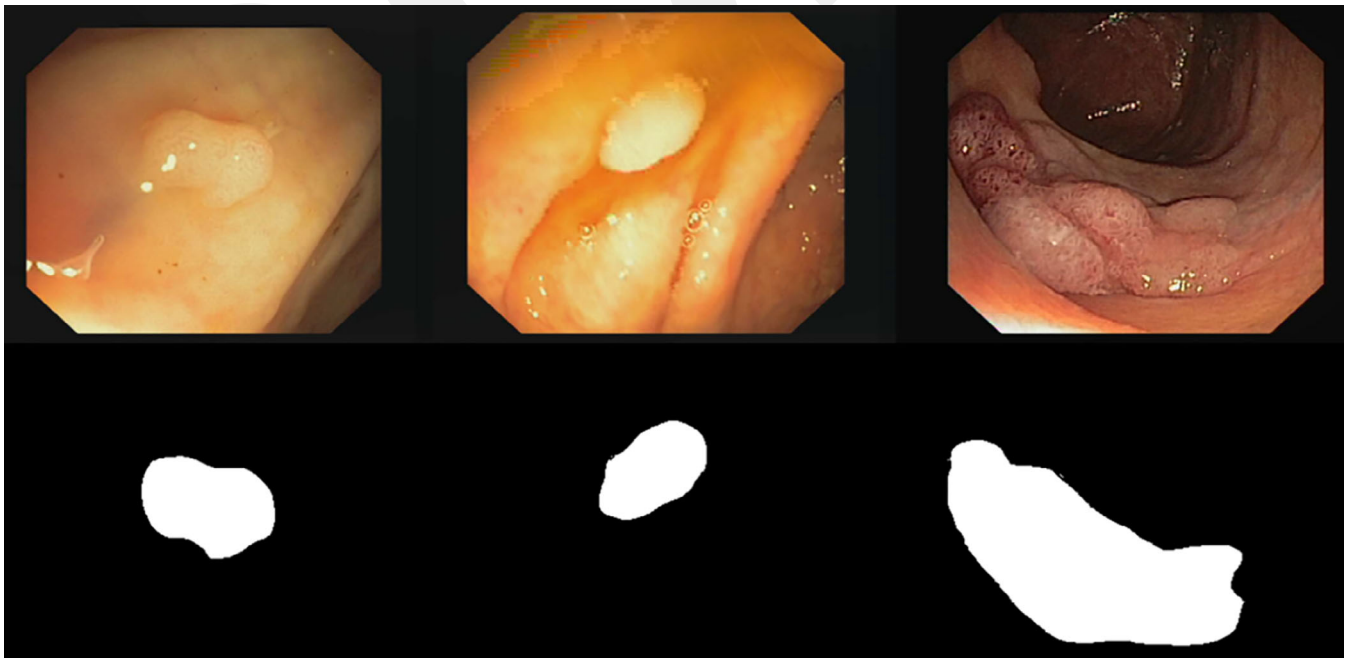


**FIGURE 1** Three different polyps and their ground truth counterparts from “CVC-ClinicDB” database [Color figure can be viewed at [wileyonlinelibrary.com](http://wileyonlinelibrary.com)]

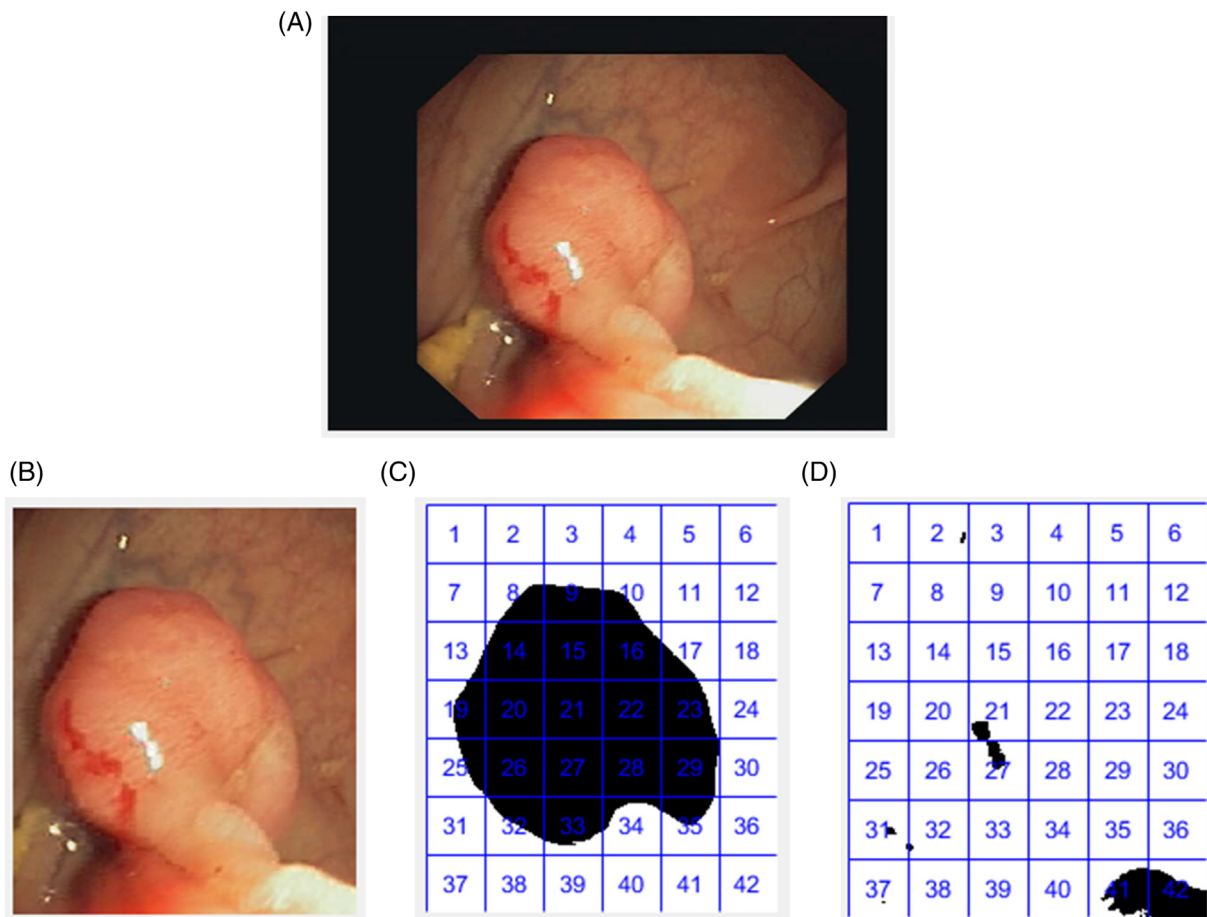


**FIGURE 2** Original image (A), cropped image (B), ground truth image (C), tiles w/Reflection (D) [Color figure can be viewed at [wileyonlinelibrary.com](http://wileyonlinelibrary.com)]



**FIGURE 3** Four different size “real” reflections added on the tiles corresponding to the reflections covering 2%, 10%, 20%, and 30% of the pixels in each tile ( $32 \times 32$  pixels)

reflections we used in our subsequent analysis which corresponded to the reflections covering 2%, 10%, 20%, and 30% of the tiles. For example, 2% and 10% reflections mean that out of 1024 pixels ( $32 \times 32$  pixels in one tile) approximately 20 and 100 pixels, respectively, were replaced with pixels containing specular reflection.

We know that specular reflections that occur on the colonoscopy images do not have a specific/regular shape. The random shape may occur due to (a) the illumination light coming onto the colon surface and/or the angle of incidence of the camera, (b) the folded structure of the colon, and (c) the continuous movement of the tube/probe during the colonoscopy procedure. Therefore, there might exist infinitely many specular reflection types with

different size, shape or characteristics. Here, we had to limit ourselves with the size of reflections, however, we chose such specular reflections that had different but nonuniform shapes, corresponding to the real situation in colonoscopy. As shown in Figure 3, the relatively small reflections we used were somewhat oval-shaped, however, as the size increased, they became more irregular.

## 2.4 | Image interpolation

In this study, we tested the effect of different image interpolation approaches on texture features which were used in the automatic classification of polyps. The image

interpolation refers to interpolating (by fitting a function) pixel values corresponding to specular reflections using the pixel values without reflection. The concept we are referring here is also called inpainting.

In this part, we applied two-dimensional (2D) nearest neighbor, bilinear, and bicubic interpolation approaches on healthy and polyp tiles (a total of 15 674 tiles) on which specular reflections were previously added as explained above. We used a built-in function called “fillmissing” in MATLAB for image interpolation. We were able to choose and apply each interpolation methodology separately using this function. In several different studies<sup>17-19</sup> researchers reported results from various interpolation approaches to remove specular reflection from endoscopic images. In the nearest neighbor interpolation, the empty spaces will be filled in with the nearest neighboring pixel value. In the bilinear interpolation, the main idea is to perform linear interpolation first in one direction, and then in the other direction. Although each step is linear in the sampled values and in the position, the interpolation as a whole is quadratic in the sample location.<sup>21-23</sup> The bicubic interpolation is a method that uses four neighboring pixels to fill the missing part of the image. For each of the neighboring four data points, we need to know its intensity value, its partial derivatives along both axes, and its cross-derivatives.<sup>24</sup> In this study, we have not used interpolation to fill missing values but to update pixels with reflections.

## 2.5 | Feature extraction

Image texture is one of the most important characteristics used to describe region of interest in an image. They are the measures of intensity variations of a surface that determine properties such as smoothness, roughness, and regularity. Texture based feature extraction methods are categorized into first order and second order techniques. First order statistics does not use neighborhood relationships, but second order statistics use neighborhood relationships.

After preprocessing, addition of specular reflections and interpolation of images with reflections, the next step was to extract image texture features. Actually, we have extracted features from the tiles with no specular reflections and from the same tiles but reflection added. By this way, we wanted to investigate *the effect of interpolation on the tiles with specular reflections in terms of texture features* and the *discrimination of healthy tiles and tiles with polyps using the extracted features*.

In order to perform feature extraction, we used three popular second order texture extraction approaches

called gray level co-occurrence matrix (GLCM), gray level run length matrix (GLRLM), neighborhood gray tone difference matrix (NGTDM), and four first order statistics, such as kurtosis, SD, energy and skewness.

The gray level co-occurrence matrix (GLCM), which describes the relationship between neighboring pixels, indicates the frequency of image brightness recurrence at a certain distance and direction. If the co-occurrence matrix is denoted by  $C$ , the value of  $C(i, j)$  specifies how many times  $i$  coincides with the value of  $j$  in some specified positional relations.  $i$  and  $j$  are the pixel value. But in general, this distance between pixels is regarded as a “one-pixel distance” and a co-occurrence matrix is formed accordingly. Some of the attributes extracted from the GLCM are autocorrelation, contrast correlation, difference, and homogeneity. Equations for the calculation of these features have not been included here since they can be found in many sources one of which is.<sup>25</sup>

In the gray level run length matrix (GLRLM) approach, a set of consecutive pixels with the same gray level value in the specified direction forms a gray level sequence. Run length is the number of pixels in each gray level sequence. The presence of a large number of neighboring pixels at the same gray level represents a coarse-grained texture, while a small number of neighboring pixels have the same gray level represents a finer texture with a faster change. If GLRLM is denoted by  $P$ , the value of  $P(i, j)$  indicates how many times the gray level  $i$  has occurred in length  $j$ . This description is for angularly different directions but the most common use is horizontal direction.<sup>26</sup> The most common of the attributes created using the GLRLM matrix are short-length emphasis (SRE gives greater importance to short sequence lengths of any gray level), long-length emphasis (LLE gives greater importance to long string lengths of any gray level), gray-level uniformity (GLU, the smallest value when the array lengths are balanced in a balanced manner), run-length uniformity (RLU, takes the smallest value when the sequence lengths are balanced).

Neighborhood gray-tone difference matrix (NGTDM) is a matrix of columns that accommodates elements up to the number of tones and allows one to extract texture-related properties. It was first proposed by Amadasun and King in 1989 and has been used in different problems. The attributes that are extracted from this vector are coarseness, contrast, busyness, complexity, and strength.<sup>27</sup>

A total of 116 texture features were extracted using the approaches above for each tile with no reflections, 2%, 10%, 20%, and 30% reflections added and interpolated.

## 2.6 | Statistical analysis on texture features

The aim of this step was to detect any statistically significant differences between texture features obtained from reflection-free tiles from the healthy and polyp parts of the images and texture features obtained from the tiles that were reflection-added and interpolated from the healthy and polyp parts of the images. We performed paired sample  $t$  test using IBM SPSS Statistics 21.0. The null hypothesis we had was that the mean difference between two sets of observations was zero. For example, the comparison of one texture feature (say gray-level uniformity obtained using the GLRLM approach) coming from 14 248 reflection-free and 2% reflection-added and interpolated tiles corresponding to the healthy parts of the image (healthy tiles). We obtained a  $P$ -value for this comparison and checked whether it was less than .05 or not. When the  $P$ -value was less than .05 we rejected the null hypothesis and concluded that there was a strong evidence against the null. We then recoded this feature as being the one affected by the interpolation on the specular reflection of this size. Next, this step was repeated for all features and reflections with different sizes (10%, 20%, and 30% of the tile was covered with reflection). The same procedure was applied the features coming from 1426 tiles with polyps. This analysis was useful to determine robust features which were affected minimally from the image interpolation approaches we have implemented in this study. Before performing paired sample  $t$  test we applied Shapiro-Wilk test for normality check, and observed an approximately normal distribution.

## 2.7 | Classification

In the final phase of this study, we have tested two different classification methods to automatically discriminate the healthy tiles from the tiles with polyp using texture features. To remind again we had a total of 15 674 tiles from 610 images. The number of tiles that were labeled as polyp and healthy was 1426 and 14 248, respectively.

The classification methods used here were  $k$  nearest neighbors ( $k$ -NN) and random forest. The aim of this part was to investigate the effect of interpolation on the texture based classification process. For this purpose, we used both reflection-free tiles and reflection-added and interpolated tiles. First, using the WEKA software the random forest and  $k$ -NN classification methods were applied to discriminate healthy tiles with no reflection from tiles with polyp with no reflection. The number of trees for the random forest approach was 100 and  $k$  value was set to 1 for  $k$ -NN classification. Later, we continued

with the classification of reflection-free healthy tiles and 2, 10%, 20%, and 30% specular reflection plus interpolation on polyp tiles. The same procedure was followed to perform classification between reflection-free polyp tiles and 2%, 10%, 20%, and 30% specular reflections plus interpolation on healthy tiles. We performed a 10-fold cross-validation for reducing the bias.

In the performance analysis of classification methods, we used overall accuracy and  $f$ -measure.  $f$ -measure is selected as the performance metric, because it is useful for class-imbalance problems like this one. The definitions of metrics known as precision, recall, and  $f$ -measure are given below in Equations (1)-(3). Precision and recall are measures for correctness and completeness, respectively. The  $f$ -measure takes the precision and the recall into account when computing the score. It can be interpreted as a harmonic mean of precision and recall.

$$\text{Precision} = \frac{TP}{TP + FP} \quad (1)$$

$$\text{Recall} = \frac{TP}{P} \quad (2)$$

$$f\text{-measure} = \frac{2}{\frac{1}{\text{precision}} + \frac{1}{\text{recall}}} \quad (3)$$

## 3 | RESULTS

As mentioned above, the  $t$  test was used to investigate the effect of interpolation on texture features. For this purpose, features obtained from reflection-free polyp tiles and interpolated polyp tiles that included different size reflections were statistically compared. This process was carried out for bilinear, nearest neighbor, and bicubic interpolation techniques separately. In addition, the same procedure was followed for healthy tiles. When the  $t$  test was applied on reflection-free (healthy and polyp) tiles and tiles that were interpolated after 2% specular reflection was added, we observed that the number of features affected significantly ( $P < .05$ ) was between 0 and 8 out of 116 features for all interpolation techniques. In addition, the number of features affected significantly by interpolation was between 15 and 86 (12%-70% of all features) for 10% reflection-added and interpolated tiles. As expected, the number of features that was affected by interpolation increased when the size of reflection increased. Table 1 depicts the results of this part. In summary, if an image includes 2% specular reflection, any interpolation technique can be effective to eliminate reflection without changing texture features significantly. However, if the reflection percentage is over

**TABLE 1** Summary of *t* test results for the comparison of features obtained from reflection free tiles and interpolated tiles that included different size reflections

| Reflection free tiles   | Tiles with specular reflection plus interpolation | Number of significantly different features ( $P < .05$ ) |    |         |
|-------------------------|---|--|----|---------|
|                         |   | Bilinear   | NN | Bicubic |
| Reflection free polyp   | Polyp 2% reflection                               | 0  | 0  | 1       |
| Reflection free polyp   | Polyp 10% reflection                              | 15   | 21 | 82      |
| Reflection free polyp   | Polyp 20% reflection                              | 29   | 28 | 83      |
| Reflection free polyp   | Polyp 30% reflection                              | 30   | 66 | 82      |
| Reflection free healthy | Healthy 2% reflection                             | 4  | 6  | 8       |
| Reflection free healthy | Healthy 10% reflection                            | 31   | 30 | 86      |
| Reflection free healthy | Healthy 20% reflection                            | 44   | 64 | 95      |
| Reflection free healthy | Healthy 30% reflection                            | 51   | 79 | 93      |

10%, using interpolation can cause deformation on texture structure. We should note that there were four features which were common to both polyps and healthy tiles, which did not change significantly from added reflection and interpolation. Three of these robust features came from the gray level co-occurrence matrix as autocorrelation, sum of squares (variance), sum of average, and energy features obtained using the first order method.

The results of the second part of this study were summarized in Table 2. The f-measure values were computed and given for the comparison of interpolation methods and classification approaches to automatically discriminate tiles with polyps from the healthy background tiles with and without specular reflection of different sizes. For both classification approaches f-measure values were higher for bicubic interpolation when compared to other two methods. As the percentage of the specular reflection increased, f-measure values increased except for two cases (bicubic interpolation increasing from 20% to 30% reflection). Random forest was found to be performing better than k-NN in all cases.

Table 3 shows the accuracy of the best f-measure results for bilinear, nearest neighbor and bicubic interpolation methods and random forest and k-NN classification approaches. The accuracy levels were approximately 90% for the discrimination of polyp tiles from the healthy tiles without any specular reflection. The accuracies went up to ~99% as we increased the reflection percentages for both classification approaches.

## 4 | DISCUSSION AND CONCLUSIONS

In this study, we tried to answer the following question: Does the interpolation of specular reflections encountered

in colonoscopic images affect the texture features to be used in the automatic detection of polyps? First, we made comparisons between texture features obtained from an image with no specular reflections and the same features obtained with synthetically added reflections with various sizes plus the interpolation. Second, we performed automatic classification between polyp and background colon based on texture features obtained from the interpolated images. In the classification phase, we did not use the image as a whole, rather  $32 \times 32$  subimages extracted from the gray-scale colonoscopic images. We can summarize our key finding as follows:

- The size of the specular reflection is an important factor. When the images include 2% reflection, interpolation could be effective. At most 0.9% and 7% of the texture features were affected significantly from the interpolation on subimages with polyps and background, respectively. However, when the reflection size was greater than 10%, the interpolation was not effective. It is worth noting that bicubic interpolation restored the texture features the most.
- In the classification of polyp and the background, the random forest approach performed better than the *k*-NN algorithm. Using WEKA software, we obtained classification results and stated the f-measure and accuracy values. The overall accuracy level was more than 92% for all interpolation methods. The results showed that there was an improvement when BC was used over other interpolation techniques for 10%, 20%, and 30% reflection.

The previous work on this problem was limited to the interpolation (or removal) of specular reflections on colonoscopic, endoscopic or other medical images. For endoscopic images, Guo et al suggested a method to

**TABLE 2** Summary of f-measure values for the comparison of interpolation methods and classification approaches to automatically discriminate tiles with polyps from the healthy background tiles with and without specular reflection of different sizes

| Reflection added on healthy tiles (%) | Reflection added on polyp tiles (%) | Random forest |       |       | k-NN  |       |       |
|---------------------------------------|-------------------------------------|---------------|-------|-------|-------|-------|-------|
|                                       |                                     | f-measure     |       |       |       |       |       |
|                                       |                                     | BL            | NN    | BC    | BL    | NN    | BC    |
| 0                                     | 0                                   | 0.376         | 0.376 | 0.376 | 0.389 | 0.360 | 0.360 |
| 0                                     | 2                                   | 0.376         | 0.383 | 0.384 | 0.352 | 0.357 | 0.352 |
| 0                                     | 10                                  | 0.376         | 0.391 | 0.835 | 0.358 | 0.374 | 0.734 |
| 0                                     | 20                                  | 0.406         | 0.474 | 0.956 | 0.407 | 0.420 | 0.931 |
| 0                                     | 30                                  | 0.450         | 0.675 | 0.872 | 0.420 | 0.576 | 0.786 |
| 2                                     | 0                                   | 0.389         | 0.390 | 0.379 | 0.370 | 0.366 | 0.365 |
| 10                                    | 0                                   | 0.411         | 0.429 | 0.829 | 0.377 | 0.389 | 0.731 |
| 20                                    | 0                                   | 0.490         | 0.571 | 0.942 | 0.427 | 0.464 | 0.893 |
| 30                                    | 0                                   | 0.585         | 0.758 | 0.864 | 0.478 | 0.612 | 0.736 |

**TABLE 3** Accuracy of the best f-measure results for bilinear, nearest neighbor, and bicubic interpolation methods

| Interpolation types | Reflection added on healthy tiles (%) | Reflection added on polyp tiles (%) | Overall accuracy |       |
|---------------------|---------------------------------------|-------------------------------------|------------------|-------|
|                     |                                       |                                     | Random forest    | k-NN  |
| No interpolation    | 0                                     | 0                                   | 92.56            | 87.88 |
| Bilinear            | 0                                     | 30                                  | 93.02            | 88.82 |
|                     | 30                                    | 0                                   | 94.21            | 90.67 |
| Nearest neighbor    | 0                                     | 30                                  | 95.13            | 92.13 |
|                     | 30                                    | 0                                   | 96.24            | 93.36 |
| Bicubic             | 0                                     | 20                                  | 99.21            | 98.75 |
|                     | 20                                    | 0                                   | 98.94            | 98.05 |

eliminate specular reflection,<sup>18</sup> Stehle used spectral deconvolution algorithm to remove reflections,<sup>19</sup> Arnold et al<sup>20</sup> and Karapetyan et al<sup>21</sup> preferred different inpainting algorithms. In addition, Tchoulack et al proposed using a real-time inpainting algorithm to eliminate specular reflections from endoscopic images.<sup>28</sup> Aydi et al showed the use of interpolation methods to remove reflections on iris images.<sup>29</sup> None of the abovementioned studies focused on the effect of these methods on the accuracy of automatic classification of the polyp and background.

We may have considered using shape features to detect polyps on the colonoscopy images<sup>16</sup> if we were to use an image as a whole. Instead, we used subimages that were cut out of the whole image in which the shape information was lost. That is why we restricted ourselves with texture features, and did not use shape features in our study.

Although we believe that our results are promising, we must acknowledge that these findings need to be validated or augmented by future studies in which more images were

included in the database. One of the limitations of this study is that we had to study with an unbalanced database. In this study, only 10% of the subimages (tiles) came from the polyps. In addition, the effect of interpolation in the detection of polyps was investigated on the subimages not the whole image. A deep learning-based approach will be developed in our laboratory to compensate for the specular reflections. Furthermore, a future study in our laboratory will tackle a real time specular reflection removal approach. We will also investigate the use of other feature extraction methods, feature selection methods and other classifiers such as SVM and ensemble techniques.

#### ACKNOWLEDGMENT

The first author RNK is supported by the Turkish Higher Education Council's 100/2000 Program as a graduate student with a monthly stipend.

#### CONFLICT OF INTEREST

The authors declare that they have no conflict of interest.

## ETHICS STATEMENT

For this type of study, formal consent is not required.

## ORCID

Rukiye Nur Kaçmaz  <https://orcid.org/0000-0002-3237-9997>

Bülent Yılmaz  <https://orcid.org/0000-0003-2954-1217>

Zafer Aydın  <https://orcid.org/0000-0001-7686-6298>

## REFERENCES

1. *Colon Cancer*. <http://www.mayoclinic.org/diseasesconditions/colocancer/home/ovc-20188216>. Accessed September 10, 2017.
2. Ong J, Seghouane A, Osborn K. Polyp detection in CT colonography based on shape characteristics and kullback-leibler divergence. *Biomed Imaging: Nano Macro*. 2008;636-639.
3. *Colorectal Polyps and Cancer*. <http://www.webmd.com/color-ectalcancer/guide/colorectal-polyps-cancer>. Accessed September 10, 2017.
4. Tajbakhsh N, Gurudu SR, Liang J. Automatic polyp detection using global geometric constraints and local intensity variation patterns. *Int Conf Med Image Comput Comput-Assisted Interv*. 2014;8674(62):179-187.
5. Hwang S, Oh J, Tavanapong W, Wong J, De Groen PC. Polyp detection in colonoscopy video using elliptical shape feature. *Proc Int Conf Image Process ICIP*. 2007;2:465-468.
6. Park M, Jin SJ, Hofstetter R, Xu M, Kang BH. Automatic colonic polyp detection by the mapping using regional unit sphere. Paper presented at Proc. 2008 Int. Conf. Multimed. Ubiquitous Eng. April 24-26, 2008; Busan, South Korea.
7. Bernal J, Sánchez J, Vilariño F. Towards automatic polyp detection with a polyp appearance model. *Pattern Recognit*. 2012;45(9):3166-3182.
8. Ong JL, Seghouane A-K. Feature selection using mutual information in CT colonography. *Pattern Recognit Lett*. 2011;32:337-341.
9. Ong JL, Seghouane A-K. From point to local neighborhood: polyp detection in CT colonography using geodesic ring neighborhoods. *IEEE Trans Image Process*. 2011;20(4):1000-1010.
10. Yoshida H, Nappi J. Three-dimensional computer-aided diagnosis scheme for detection of colonic polyps. *IEEE Trans Med Imaging*. 2001;20(12):1261-1274.
11. Tajbakhsh N, Chi C, Gurudu SR, Liang J. Automatic polyp detection from learned boundaries. Paper presented at: IEEE 11th Int. Symp. Biomed. Imaging, 2014; 97-100.
12. Wang P, Krishnan SM, Kugean C, Tjoa MP. Classification of endoscopic images based on texture and neural network. *Annu Reports Res React Inst, Kyoto Univ*. 2001;4:3691-3695.
13. Tjoa MP, Krishnan SM. Feature extraction for the analysis of colon status from the endoscopic images. *Biomed Eng Online*. 2003;2(1):9.
14. Alexandre LA, Casteleiro J, Nobre N. Polyp detection in endoscopic video using SVMs. Paper presented at: KPKDD Proc. 11th Eur. Conf. Princ. Pract. Knowl. Discov. Databases; September 2007; Berlin Heidelberg: Springer-Verlag.
15. Ghosh T, Fattah SA, Shahnaz C, Kundu AK, Rizve MN. Block based histogram feature extraction method for bleeding detection in wireless capsule endoscopy. Paper presented at: TENCON 2015 – 2015 IEEE Region 10 Conference; November 1-4, 2015; Macao.
16. Karkanis SA, Iakovidis DK, Maroulis DE, Karras DA, Tzivras M. Computer-aided tumor detection in endoscopic video using color wavelet features. *IEEE Trans Inf Technol Biomed*. 2003;7(3):141-152.
17. Benäçeo M, Hudec R. Novel method for color textures features extraction based on GLCM. *Radioengineering*. 2007;16(4):64-67.
18. Guo JJ, Shen DF, Lin GS, Huang JC, Liu KC, Lie WN. A specular reflection suppression method for endoscopic images. *Proc. 2016 IEEE 2nd Int. Conf. Multimed. Big Data, BigMM 2016*, pp. 125-128; 2016.
19. Stehle TH. Specular reflection removal in endoscopic images. *Proc. 10th Int. Student Conf. Electr. Eng. Poster*; July, p. 6; 2006.
20. Ghosh A, Arnold M, Ameling S, Lacey G. Automatic segmentation and inpainting of specular s for endoscopic imaging. *Eurasip J Image Video Process*. 2010;2010:1-12.
21. Karapetyan G, Sarukhanyan H. Automatic detection and concealment of specular reflections for endoscopic images. *9th Int. Conf. Comput. Sci. Inf. Technol. Revis. Sel. Pap.*; 2013.
22. Bernal J, Sánchez FJ, Fernández-Esparrach G, Gil D, Rodríguez C, Vilariño F. WM-DOVA maps for accurate polyp highlighting in colonoscopy: validation vs. saliency maps from physicians. *Comput Med Imaging Graph*. 2015;43:99-111.
23. Olivier R, Hanqiang C. Nearest neighbor value interpolation. *Int J Adv Comput Sci Appl*. 2012;3(4):25-30.
24. <https://www.mathworks.com/>
25. Ergen B, Baykara M. İstatistiksel uzaysal alan metotlarının içerik tabanlı tıbbi görüntü erişimi için bir uygulama. *Fırat Üniv Mühendislik Bilimleri Dergisi*. 2011;23(2):87-93.
26. Sonka M, Hlavac V, Boyle R. *Image Processing, Analysis, and Machine Vision*. United States: International Thomson Publishing; 1999.
27. Amadasun M, King R. Textural features corresponding to textural properties. *IEEE Trans Syst Man Cybern*. 1989;19(5):1264-1274.
28. Tchoulack S, Langlois JMP, Cheriet F. Cheriet, A video stream processor for real-time detection and correction of specular reflections in endoscopic images, Paper presented at: 2008 Joint 6th International IEEE Northeast Workshop on Circuits and Systems and TAISA Conference; June 22-25, 2008. Montreal, QC.
29. Aydi W, Masmoudi N, Kamoun L. New corneal reflection removal method used in iris recognition system. *Int J Electron Commun Eng*. 2011;5(5):697-700.

**How to cite this article:** Kaçmaz RN, Yılmaz B, Aydın Z. Effect of interpolation on specular reflections in texture-based automatic colonic polyp detection. *Int J Imaging Syst Technol*. 2020; 1–9. <https://doi.org/10.1002/ima.22457>